Top Curr Chem (2012) 306: 89–118
DOI: 10.1007/128_2011_162

Published online: 20 May 2011

Solid-State ^{19}F-NMR of Peptides in Native Membranes

Katja Koch, Sergii Afonin, Marco Ieronimo, Marina Berditsch, and Anne S. Ulrich

Abstract To understand how membrane-active peptides (MAPs) function *in vivo*, it is essential to obtain structural information about them in their membrane-bound state. Most biophysical approaches rely on the use of bilayers prepared from synthetic phospholipids, i.e. artificial model membranes. A particularly successful structural method is solid-state NMR, which makes use of macroscopically oriented lipid bilayers to study selectively isotope-labelled peptides. Native biomembranes, however, have a far more complex lipid composition and a significant non-lipidic content (protein and carbohydrate). Model membranes, therefore, are not really adequate to address questions concerning for example the selectivity of these membranolytic peptides against prokaryotic vs eukaryotic cells, their varying activities against different bacterial strains, or other related biological issues.

Here, we discuss a solid-state ^{19}F-NMR approach that has been developed for structural studies of MAPs in lipid bilayers, and how this can be translated to measurements in native biomembranes. We review the essentials of the methodology and discuss key objectives in the practice of ^{19}F-labelling of peptides. Furthermore, the preparation of macroscopically oriented biomembranes on solid supports is discussed in the context of other membrane models. Two native biomembrane systems are presented as examples: human erythrocyte ghosts as representatives of eukaryotic cell membranes, and protoplasts from *Micrococcus luteus* as membranes

K. Koch, M. Ieronimo, and M. Berditsch
Institute of Organic Chemistry and CFN, Karlsruhe Institute of Technology (KIT), Fritz-Haber-Weg 6, 76131 Karlsruhe, Germany

S. Afonin
Institute of Biological Interfaces (IBG-2), Karlsruhe Institute of Technology (KIT), P.O.B. 3640, 76021 Karlsruhe, Germany

A.S. Ulrich (✉)
Institute of Organic Chemistry and CFN, Karlsruhe Institute of Technology (KIT), Fritz-Haber-Weg 6, 76131 Karlsruhe, Germany
and
Institute of Biological Interfaces (IBG-2), Karlsruhe Institute of Technology (KIT), P.O.B. 3640, 76021 Karlsruhe, Germany
e-mail: anne.ulrich@kit.edu

from Gram-positive bacteria. Based on our latest experimental experience with the antimicrobial peptide gramicidin S, the benefits and some implicit drawbacks of using such supported native membranes in solid-state ^{19}F-NMR analysis are discussed.

Keywords Solid-state NMR structure analysis · 19F-labeling · Membrane-active peptides · Native biomembranes · Oriented membrane models · Antimicrobial peptides

Contents

1 Introduction: Towards *In-Cell* NMR

There are several advantages to studying proteins *in-cell*, instead of analyzing them *in vitro* or in crude lysates. The presence of a natural environment obviously brings about the genuinely relevant structures and it may modulate the molecular interactions and overall behaviour of a protein. For various reasons, it may not be possible to imitate these aspects adequately *in vitro*. Another advantage is the ability to study proteins that are difficult to purify or unstable outside the cellular surrounding. It may even be advantageous to introduce externally prepared proteins into eukaryotic cells. This allows the analysis of complex biological processes, like signalling cascades, protein turnover cycles and stimulus-responsive post-translational modifications, and may even lead to the discovery of new metabolic pathways [1–3]. A recent remarkable example of the power of *in-cell* NMR *in acto* is the 3D structure determination of the putative heavy-metal binding protein TTHA1718 from *Thermus thermophilus* HB8, which was overexpressed in living *Escherichia coli* and solved exclusively on the basis of *in-cell* NMR data [4].

When placed into an NMR spectrometer, a biological sample is examined essentially without perturbations. NMR structures are considered as native, as the method does not interfere with metabolically relevant conformational changes, binding events, post-translational modifications, or dynamic features of the protein [5]. The only potentially perturbing factors in an experiment are the presence of static and oscillating magnetic fields, and sample heating due to radiofrequency-driven or

mechanical rotation [6, 7]. The heating effects can be compensated, and their impact is anyhow significantly lower than the radiation damage associated with crystallography or high-resolution microscopy. As NMR observation is perfectly compatible with living organisms, as in magnetic resonance imaging (MRI), and causes no degradation of macromolecules, this technique is considered as truly non-invasive. Naturally, NMR is the prime candidate to solve detailed 3D molecular structures non-invasively *in-cell*.

In the above-mentioned study of the protein TTHA1718, the authors also reported the problems they faced, namely significant instability of the cell culture, and low NMR signal intensities [4]. The latter illustrates the principal disadvantage of the technique: an intrinsically low sensitivity. Some improvements in the short term are expected, i.e. based on improved hardware (higher magnetic fields, alternative designs of probe-heads), on software advancements (sparse data acquisition, maximum-entropy signal deconvolution), and especially on recent developments in metabolic isotope-labelling strategies, and mediated signal enhancements such as dynamic nuclear polarisation (DNP) [8]. Though highly encouraging, these improvements are not yet able to overcome routinely the sensitivity problem, hence certain manipulations of a sample before the measurement are usually unavoidable. These include the preparation of densely packed cell pellets, the use of deficient growth media for isotope enrichment, or anabolic conditions to overexpress a protein. Such treatments cause some stress on the cells, hence the absolute non-invasiveness of NMR has been questioned [9, 10]. Nevertheless, these effects are comparable to the stresses induced by the mechanical, electric or chemical treatments applied by other methods of observing living cells. Concerning the structure analysis contest between spectroscopic and scattering methods, the latter are mostly challenged by solving structures of weak oligomeric complexes and membrane proteins, which tend to be inaccessible to NMR due to their large size. Notably, with the development of milder crystallization conditions, the traditionally artefact-prone scattering methods are progressively placing the proteins into more biomimetic environments. At the same time, the intrinsically non-invasive NMR methods seemingly move towards more perturbing sample pre-treatments like DNP or ^{19}F-labelling to increase sensitivity [11].

Faced with low sensitivity, the first *in-cell* NMR experiments were logically performed in cells with high native protein concentrations, such as haemoglobin in erythrocytes [12]. Next, *in-cell* NMR was demonstrated on organisms like *E. coli*, which could be readily genetically manipulated overexpress the desired protein [1, 13]. At the same time, isotope-labelled proteins have been introduced into cultured cells using mechanical microsyringe injections, electroporation or carrier-mediated delivery [1–4, 14]. These methods tend to be limited to specific cell types, e.g. microinjection is applicable to large oocytes and carrier-mediated delivery is successful in cells with high constitutive levels of endocytosis, such as immortalized cancer cell lines.

The current state of *in-cell* NMR has been recently reviewed [5, 9], and it appears that genuine non-invasive NMR measurements of any protein of interest in any cell type will be achievable only in the mid-term future. However, the

promise of such experiments as an ultimate scientific goal provides a strong driving force for the immediate progress of biological NMR. One step towards this scientific vision, i.e. the structural characterization of a protein under native conditions, is the subject of this contribution. We will specifically discuss the progress of solid-state NMR (ssNMR) applied to ^{19}F-labelled membrane-active peptides (MAPs) when bound to native biomembranes in macroscopically oriented samples.

2 Solid-State ^{19}F-NMR

The traditional power of liquid-state NMR is the characterization of molecular structures to atomic-resolution, and the simultaneous access to dynamic information on various time-scales. For proteins in solution such a dynamic view is particularly relevant and unique for partially unfolded sequences, as well as for conformational interchanges, e.g. during catalysis. Proteins that are associated with biomembranes, on the other hand, are not readily accessible by liquid-state NMR unless they are relatively small and stably folded in detergent micelles. The only way to study membrane proteins in a quasi-native lipid bilayer is provided by ssNMR. Besides membrane protein structure analysis, ssNMR is particularly powerful in addressing the lipid interactions of MAPs, and characterizing other types of non-crystalline complexes such as amyloid fibrils [15–21]. Given the fluid nature of a liquid crystalline membrane, special attention has to be paid to the dynamic behaviour of membrane-bound peptides and proteins. The following sections will be devoted to their ssNMR analysis in macroscopically oriented membrane samples. Magic-angle-spinning (MAS) NMR methods will not be discussed here, as the samples usually need to be cooled down below the lipid phase transition or frozen to sub-zero temperatures. The significant morphological changes in both the lipidic as well as peptidic components suggest that the resulting structural MAS NMR data are less meaningful in a biological context.

MAPs exhibit a wide range of different biological functions, such as antimicrobial, cell-penetrating and fusogenic. The interested reader is referred to the recent *Special Issue* of the *European Biophysics Journal* [22] in which diverse examples are presented. MAPs are typically short, cationic, and unstructured in aqueous solution. In the membrane-bound state, however, they tend to fold into simple well-defined 3D structures (such as an α-helix) with an overall amphiphilic character. Discrete steps of oligomerization and self-assembly have been reported and seem to reflect the functional mechanism of these peptides, such as pore-formation in the bilayer. Many MAPs are also known to undergo dramatic conformational changes as a response to the environment, i.e. they exhibit a pronounced structural plasticity when converting, e.g. from a monomeric α-helix to a β-pleated aggregate. Hence, although easy to obtain, atomic structures of MAPs as determined by liquid-state NMR or X-ray diffraction tend to have only limited relevance with regard to their biological mode of action. Once the 3D conformation has been established, the critical structural information is related to alignment of the molecule in the

membrane, to its depth of immersion, to its oligomeric state and to its overall dynamic behaviour as a response to changes in the environment (e.g. peptide concentration, temperature, lipid composition, pH, ionic strength, presence of other membrane-bound components, etc.). When studying a MAP in action, at least two situations have to be considered – the unbound state in solution and the membrane-bound structure – which are interrelated by the specific binding affinity under the given conditions. The second situation is technically very challenging because an adequate membrane environment is required. Here, ssNMR appears to be the only method that is capable of revealing the genuine structural behaviour of an MAP at quasi-atomic resolution, even in a native biomembrane and possibly in the context of a living cell [19, 21, 23–25]. For this type of application alone, ssNMR can be expected to be heavily used, since the number of known MAPs is in the thousands, with further hundreds of thousands of sequences predicted and as yet unexplored [26–29].

In ssNMR the problem of low sensitivity prevails and is especially severe, as the spectral lines are much broader and the signal-to-noise levels are orders of magnitude lower than in liquid-state NMR. The use of macroscopically oriented samples alleviates this problem to some extent, but cannot reach the comparatively narrow line-widths of typical MAS spectra. Yet, a fundamentally simple and elegant way to overcome the sensitivity issue is the use of selective ^{19}F-labels [30–32], taking advantage of the high gyromagnetic ratio of the fluorine nucleus. For MAPs in particular, ^{19}F-NMR enables unprecedented sensitivity, in practice about 20-fold higher than for ^{2}H-NMR and 100-fold better than ^{15}N-NMR in comparable samples [33, 34]. Only a fraction of a milligram is needed to record a ^{19}F-NMR spectrum, i.e. 0.25 mg of a selectively labelled 20-amino acid peptide can be typically measured in about 1 h. This remarkable sensitivity gives unique access to ssNMR studies of peptide-to-lipid ratios of down to 1/3000 in model membranes, and in principle even to background-free *in-cell* observation. As the methodological aspects have been reviewed before [35–37], here we will only briefly present the major arguments behind the use of ^{19}F-NMR from a biological point of view, and then focus on the peculiarities of selective ^{19}F-labelling of MAPs.

The fluorine nucleus possesses a very high magnetic moment (81% of ^{1}H), leading to exquisite NMR sensitivity and strong dipolar couplings. A spin of 1/2 keeps the ssNMR spectral lineshapes simple, as there are no quadrupolar contributions. The absence of a natural background in biological samples, together with the 100% natural abundance, advertises ^{19}F for selective labelling – especially under *in-cell* conditions which suffer from an enormous ^{13}C natural abundance background and even considerable intensity from ^{2}H. Owing to the lone pairs of electrons on a fluorine substituent, its isotropic chemical shift (CS) has a much broader range than ^{1}H, and it is rather sensitive to the local environment. Being dependent on temperature, pH, solvent and dielectric environment, the CS can be used to monitor these parameters [32, 34, 38]. However, in the present applications of ^{19}F-NMR to MAPs in oriented membrane samples, we will focus entirely on the anisotropy, i.e. the orientation-dependence of the CS and of the dipolar couplings.

^{19}F-labelling has been explored, amongst other signal-enhancement strategies, for *in-cell* NMR studies as early as 1989 [39] and continues to be used for proof-of-principle demonstrations to date [40]. There are several inherent difficulties associated with the use of this particular nucleus, however. The first type is purely of a technical nature, as the ^{19}F- and ^{1}H-NMR frequencies are close to one another, especially at low magnetic field strength. High-performance rf-filters are therefore required on both NMR channels (^{1}H/^{19}F), which are fortunately now available commercially [41–43]. Likewise, the stringent necessity to use custom-made Teflon-free NMR-probes and electronics has been alleviated by designated commercial hardware, yielding essentially background-free spectra. Another, less obvious, aspect is the considerable risk of introducing a chemical ^{19}F-contamination during sample preparation. Especially when working with synthetic peptides, or even with natural materials that have been purified by HPLC, traces of fluorinated solvents (trifluoroethanol, hexafluoro-2-propanol) or synthetic reagents (trifluoroacetic acid) may remain in the sample and actually dominate the NMR spectrum. In our experience, this problem can only be completely eliminated by designating a "fluoro-solvent-free" zone in the lab, comparable to the typical "protease-free" or "nuclease-free" areas in a bio-lab. Even though the removal of TFA has been reported [44, 45], we rarely found this approach to give satisfactory results.

2.1 NMR of Oriented Membranes

ssNMR structure analysis of MAPs in macroscopically oriented samples is based on the simple principle that all membrane-bound molecules are aligned the same way relative to the bilayer normal. The sample is placed into the spectrometer such that its unique axis is parallel to the static magnetic field. This way, the orientational dependence of the chemical shift anisotropy (CSA) and/or the dipole–dipole interaction (DD) (or the quadrupolar anisotropy in case of ^{2}H) directly reveals the alignment of the NMR label. In the present context a single ^{19}F-substituent or a CF_3-group is observed, but the same principle applies to ^{2}H-NMR (works well for $^{2}H_3$-alanine) and ^{15}N-NMR (works well for uniformly backbone-labelled helices). The most suitable ^{19}F-NMR reporter is in fact the CF_3-group, which is always engaged in fast rotation around the C–CF_3 axis at room temperature. The characteristic feature to be measured is the angle θ between the C–CF_3 axis and the spectrometer magnetic field, which obeys the simple relationship $DD \propto 3\cos^2\theta - 1$ (see Fig. 1a). The splitting DD is taken from the NMR spectrum, which has a triplet lineshape consisting of both the axially symmetric ^{19}F–^{19}F dipolar coupling and an axially symmetric CSA (see Fig. 2c). The CSA of a *mono*-fluoro substituent, on the other hand, is axially non-symmetric and therefore can no longer be described by a unique angle θ. Another advantage of the CF_3-group is the fact that the dipolar splitting can be directly read off a single-pulse 1D spectrum, which needs to be referenced (as has to be done for the CSA). The intrinsically unknown sign of DD can be readily determined from the simultaneous spectral shift associated with the

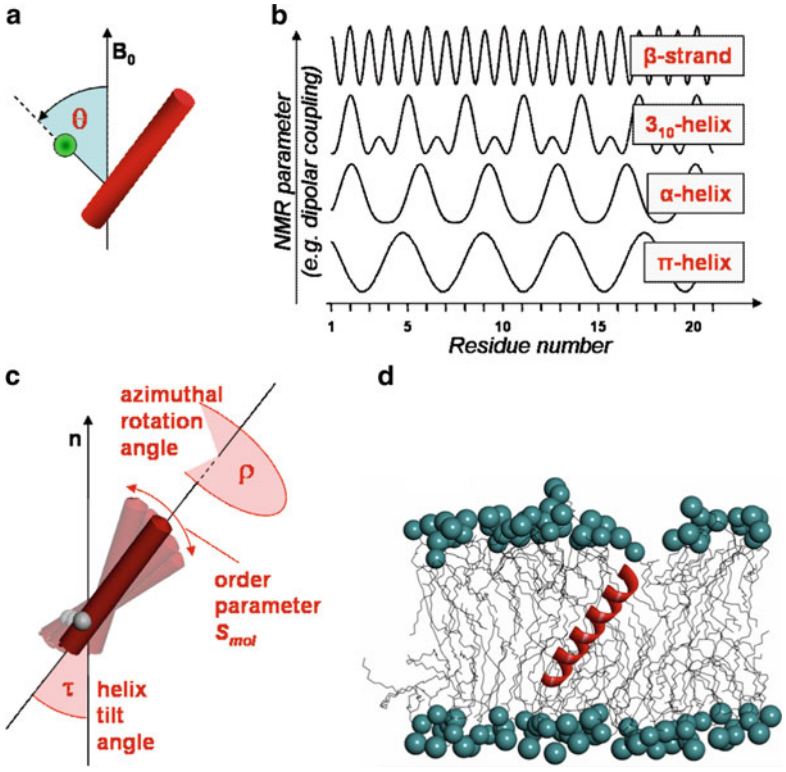

Fig. 1 Solid-state NMR structure analysis relies on the ^{19}F-labelled peptides being uniformly embedded in a macroscopically oriented membrane sample. (**a**) The angle (θ) of the ^{19}F-labelled group (e.g. a CF_3-moiety) on the peptide backbone (shown here as a *cylinder*) relative to the static magnetic field is directly reflected in the NMR parameter measured (e.g. DD, see Fig. 2c). (**b**) The value of the experimental NMR parameter varies along the peptide sequence with a periodicity that is characteristic for distinct peptide conformations. (**c**) From such wave plot the alignment of the peptide with respect to the lipid bilayer normal (n) can then be evaluated in terms of its tilt angle (τ) and azimuthal rotation (ρ). Whole-body wobbling can be described by an order parameter S_{mol}. (**d**) The combined data from several individual ^{19}F-labelled peptide analogues thus yields a 3D structural model of the peptide and how it is oriented in the lipid bilayer

CSA [46]. The local alignment of a peptide segment can thus be described by a C–CF_3 vector that protrudes in a well-defined way from the α carbon on the backbone (see Sect. 2.2 on ^{19}F-labelled amino acids).

Several local labels need to be measured, usually one-by-one in individual samples in the case of ^{19}F-NMR. The combined set of anisotropic NMR parameters then allows one to re-construct the geometry of the entire peptide and to determine its alignment in the membrane, as illustrated in Fig. 1 [35–37, 47, 48]. The only prerequisite is that the ^{19}F-labelled moiety has to be rigidly attached to the peptide backbone, and that the peptide assumes a well-defined secondary structure. Provided that a sufficient number of local orientational constraints can be measured

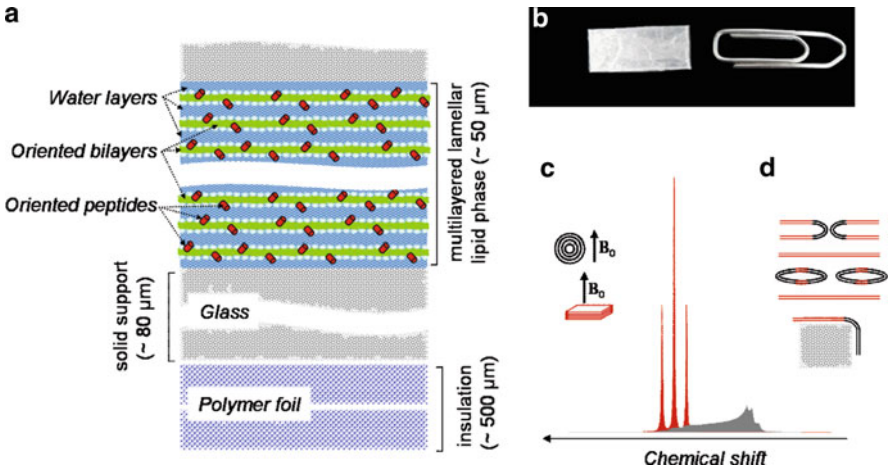

Fig. 2 Mechanically oriented bilayer samples as a membrane model for ssNMR. (**a**) Illustration of the hydrated lipid bilayers with MAPs embedded, the glass supports, and the insulating wrapping. (**b**) A real sample consists of 15 stacked glass slides. (**c**) Schematic solid-state ^{19}F-NMR lineshapes from an oriented CF_3-labelled peptide (*red*), and the corresponding "powder" lineshape from a non-oriented sample (*grey*). (**d**) Illustration of typical orientational defects in real samples – the sources of "powder" contribution in the spectra

(usually ≥ 3), it is possible to calculate not only the tilt-angle (τ) and the azimuthal rotation (ρ) of such a secondary structure element, but also to describe its wobbling in terms of an order parameter S_{mol} ($0 \leq S_{mol} \leq 1$). When four or more independent constraints are available, the whole-body dynamics can in principle be evaluated in terms of an extended dynamical model [49–51]. The least-squares fitting procedure can best be visualized by plotting the experimental NMR data (DD or CSA) against the residue number of the peptide sequence. A wave-like pattern will be obtained with a repetition after 3.6 residues for an α-helix, 3 residues for a 3_{10}-helix, 4 for a π-helix, or 2 for a β-strand (see Fig. 1b). It is thus straightforward to find out which secondary structure is compatible with the experimental data and which conformations can be excluded [35, 48]. The best-fit solution then yields at the same time the values of τ, ρ and S_{mol}, which fully describe the orientation of the peptide with respect to the membrane normal. In this way, the membrane-bound structures of several different types of MAPs have been resolved over recent years [46, 52–54]. Notably, a peptide that does not bind at all and rather diffuses freely in the aqueous layer will produce exclusively isotropic signals. A non-ordered or aggregated peptide, on the other hand, will reveal itself by producing so-called "powder"-lineshapes in an oriented sample.

For the orientation-based structure analysis of MAPs, uniformly oriented lipid bilayers are typically prepared on solid supports as illustrated in Fig. 2 [23, 47, 55]. These mechanically oriented membranes are advantageous for static ssNMR experiments, as they provide a robust way to orient a sample with any desired lipid composition, peptide concentration, and at any desired temperature. The lipids

and the ^{19}F-labelled MAP are usually co-dissolved in an appropriate organic solvent, spread onto a number of glass plates, and stacked after evaporation of the solvent. Oriented bilayers are spontaneously formed when this stack is equilibrated in a humid atmosphere (typically 96% relative humidity over a saturated K_2SO_4 solution), and finally it has to be wrapped in a water-impermeable foil to maintain the hydration level [34, 37, 56, 57]. Alternatively, when working with delicate or aggregation-prone peptides, oriented samples can be formed from aqueous suspensions of liposomes into which the peptide has been reconstituted by detergent dialysis. In this case the suspension is deposited onto the support slide, and excess water is removed by equilibration in a hydration chamber. During this process the vesicles fuse and align on the slide as flat multi-bilayers.

2.2 *^{19}F-Labelling of Peptides*

Compared to conventional NMR isotopes (^{13}C, ^{15}N, ^{2}H), ^{19}F-labels cannot be readily placed into proteins in a versatile manner by any biosynthetic expression strategy. Certain auxotrophic bacterial strains can be used to incorporate *iso*-steric ^{19}F-labelled amino acids (e.g. Fluoro-Phe, Fluoro-Trp, Fluoro-Leu, Fluoro-Ile; see Fig. 3), but yields tend to be low. Many other fluoro-organics are toxic if they get converted into fluoroacetic acid, which blocks the enzyme aconitase in the citric

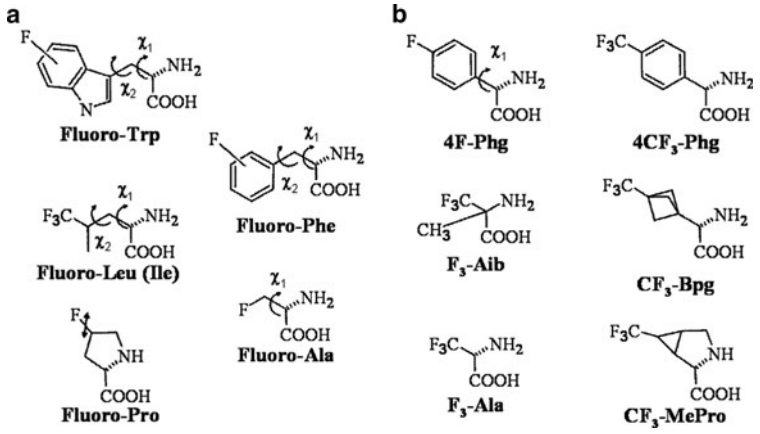

Fig. 3 Important ^{19}F-labelled amino acids. (**a**) Compounds that are *iso*-steric to native amino acids can be incorporated into proteins biosynthetically, but they possess too many degrees of torsional freedom to be useful for ssNMR structure analysis. (**b**) In these artificial amino acids the ^{19}F-reporter group is rigidly attached to the peptide backbone. They can be incorporated by solid-phase peptide synthesis, but some problems can arise due to racemisation (4F-Phg, 4CF_3-Phg), steric hindrance of coupling (F_3-Aib) or HF elimination (fluoro-Ala, F_3-Ala). 4F-Phg is additionally problematic due to an ambiguity of the side-chain rotamer. The preferred ^{19}F-labels for ssNMR structure analysis are CF_3-Bpg and CF_3-Phg (as suitable substitutes for Leu, Ile, Met, Val and Ala), as well as F_3-Aib and CF_3–MePro

acid cycle. Alternative ways of obtaining large ^{19}F-labelled proteins are by means of native chemical ligation, or by cell-free biosynthesis and semi-synthetic approaches based on an extended genetic code [58–60]. Even though the yields are still low, there is hope that methodological progress will favour these alternative routes in the not-too-distant future.

Notably, when aiming to produce short MAPs, their biosynthetic production tends to be particularly difficult anyhow. One reason is that the short mRNA is rapidly degraded, such that recombinant expression is often only possible as a fusion construct together with a large protein. On top of that, many amphiphilic MAPs are intrinsically prone to cause membrane lysis, and organisms like *E. coli* cannot usually cope with such toxic effects. Therefore, when at all possible, a fresh recombinant ^{19}F-labelling of MAPs would only make sense when an *iso*-steric ^{19}F-amino acid is to be incorporated. However, as these are too pliable to be used for the ssNMR approach outlined (see below), chemical peptide synthesis remains the best option. In principle, the covalent addition of a fluorinated moiety to an existing peptide or protein (via SH-, COOH-, or NH_2-groups) could enhance the repertoire of ^{19}F-labels, but these groups, too, are inappropriate for structure analysis.

Solid-phase peptide synthesis is the method of choice to produce polypeptides of up to 50 amino acids, especially in the case of MAPs. Any unnatural amino acid can be introduced, and recent developments in fully automated and microwave-assisted instruments allow even some less reactive or sterically confined compounds to be coupled [35, 61–63]. When selecting or designing a ^{19}F-amino acid as a label for ssNMR, several criteria have to be met. (a) For structure analysis in oriented membranes the ^{19}F-reporter group has to be rigidly attached to the Cα atom of the peptide backbone. This is a fundamental prerequisite to be able to translate the local angle θ of the label into the overall geometry and alignment of the peptide (see Fig. 1). (b) The ^{19}F-labelled amino acid must not compromise the conformation or biological action of the peptide, hence the substitution should maintain the secondary structure propensity, steric size and polarity. (c) The ^{19}F-labelled amino acid should be stable under conditions of peptide synthesis. In view of all these restrictions, it is obvious why only very few out of the many known ^{19}F-labelled amino acids can be used for ssNMR. Adequate substituents have been demonstrated for Leu, Ile, Met, Val, Ala, Aib, and more recently also Pro [53, 61, 64].

Commercially available 4F-Phg was historically the first label used to develop the basic ssNMR approach on the fusogenic peptide B18 and on antimicrobial gramicidin S (GS) (see Fig. 4 for sequences) [52, 65, 66]. From nine individual substitutions, the B18 peptide was shown to assume a "boomerang"-like helix-loop-helix structure in the membrane. In the case of GS, four positions were used, though in principle two are sufficient thanks to the symmetrical cyclic backbone. Given the latent ambiguities of single ^{19}F-substituents, CF_3-Phg were introduced and their advantages demonstrated for the helical antimicrobial peptide PGLa [46]. Four ^{19}F-labelled PGLa analogues were used to determine the molecular conformation and to describe several different alignment states in the membrane. Depending on the sample conditions, this representative α-helical peptide is able to bind flat to the membrane surface, to insert into the bilayer with an oblique tilt angle, and to assume an upright transmembrane

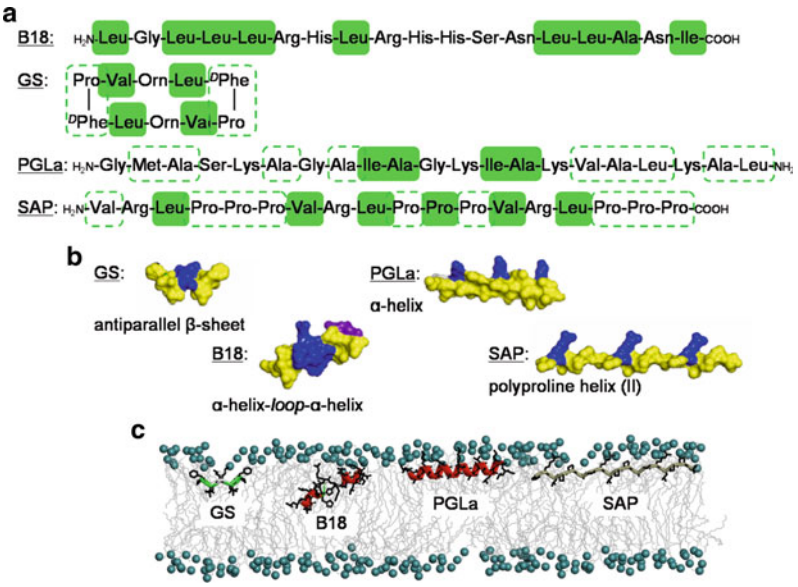

Fig. 4 Representative membrane-active peptides that have been studied by solid-state ^{19}F-NMR. (**a**) The primary sequences show which positions were substituted (*filled green boxes*) or which ones could in principle be substituted (*dotted green lines*). (**b**) Characteristic conformations of the peptides in the membrane-bound state. The space-filling solvent-accessibility models emphasize the amphiphilicity by colouring hydrophobic residues in *yellow* and cationic side-chains in *blue*. (**c**) Observed structures and alignment states of the peptides as determined by ^{19}F-NMR

alignment that is presumably responsible for pore formation. These intriguing ^{19}F-NMR results were found to be in excellent agreement with an independent ^{2}H-NMR analysis based on entirely non-perturbing $^{2}H_3$-Ala substitutions [33].

As a further improvement in the development of ^{19}F-labels, CF_3-Bpg was specifically designed and custom-made for ^{19}F-NMR. Again, PGLa was used to demonstrate the ideal properties of this novel label. This amino acid has since become a "gold standard" for ^{19}F-NMR of MAPs and been applied to several different types of peptides [54, 64, 67–69]. Likewise, F_3-Aib in both *R*- and *S*-configurations has been introduced as an ideal label for peptaibols, with alamethicin as a representative example [70]. Most recently, CF_3–methano-proline with a rigidified ring has been prepared and is currently being explored as a ^{19}F-label in the proline-rich peptide SAP [53].

3 Lipid Model Membranes

To study the structural behaviour of MAPs, an adequate membrane model (see Fig. 5) is essential. Simple organic solvent systems, such as DMSO, MeOH/H_2O or TFE/H_2O mixtures, present a similar dielectric environment as a membrane on

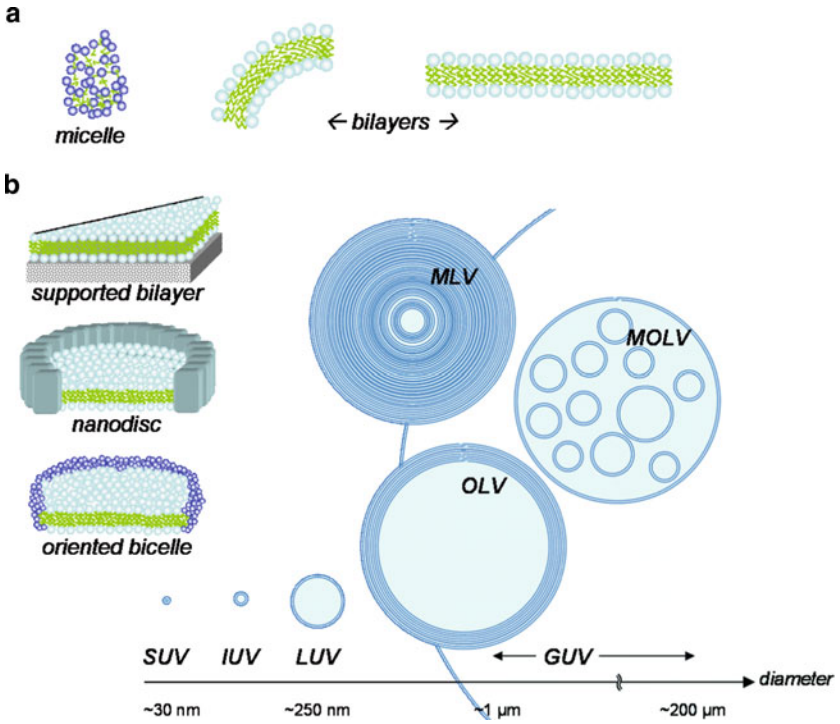

Fig. 5 Membrane models for NMR structure analysis. (**a**) An isotropic detergent micelle (*left*) is compared to the dimensions of lipid bilayers (*right*). (**b**) Macroscopically oriented membrane samples can be prepared on solid support, as nanodiscs, or as magnetically oriented bicelles. (**c**) Nomenclature and variability of liposomes: small (SUV, 20–40 nm), intermediate (IUV, 40–60 nm), large (LUV, 100–400 nm), and giant unilamellar vesicles (GUV, ~1 µm); multi-lamellar (MLV), oligo-lamellar (OLV) and highly heterogeneous multi-oligo-lamellar vesicles (MOLV)

average, and tend to favour H-bond formation. Though perfectly suitable for many spectroscopic techniques, including liquid-state NMR [71, 72], and even extendable to an ssNMR situation by freezing the solution [73, 74], such models obviously fall a long way short of an anisotropic lipid bilayer environment. Spherical detergent micelles exhibit a diffuse membrane–water interface and a hydrophobic core, hence an overall dielectric gradient is present [75–77]. However, their high radius of curvature makes it difficult to assess the membrane alignment of a peptide, and structural aspects related to higher-order peptide–peptide interactions such as pore-formation cannot be addressed either. The former problem is alleviated by the use of isotropic bicelles [78–80], which are prepared from a mixture of a long-chain lipid and a short chain detergent (such as SDS, DPC, CHAPSO or DHPC) with a molar ratio $q < 1$ and concentrations of ~10–15 wt% [81, 82]. Small isotropic bicelles are increasingly used in liquid-state NMR, empirically providing better

spectra. In most cases when using micelles, however, solubilization is the prime aim, though words of caution have been raised [83]. Isotropic detergent assemblies are often visualized with a definite shape, even as a rigid ball (oblate or prolate at best), in which the peptide or protein is immersed [84, 85]. In reality, though, micelles possess neither well-defined hydrophobic nor stable surface dimensions, as the detergent molecules rather adjust themselves around the hydrophobic part of the protein or peptide. Micelles are therefore perfect solubilizing agents for transmembrane segments, but of limited use in characterizing amphiphilic MAPs.

A different scenario is encountered with large planar bicelles, e.g. of DMPC/DHPC with a typical molar ratio $q > 3$ in suspensions of 15–25 wt%, which are often depicted as pancakes but may also look like a stack of cylindrical micelles or a slice of Swiss cheese [86–88]. These assemblies can orient themselves macroscopically in the strong magnetic field of an NMR spectrometer within a certain temperature window. Due to the magnetic susceptibility of the lipid acyl chains, the bilayer normal will usually be aligned at right angle to the field axis, but they can be flipped parallel by the addition of lanthanide ions [47, 86, 89]. This latter type of membranous sample is particularly well suited to measure anisotropic ssNMR parameters with a structural approach that has been outlined in Sect. 2.1 for the case of mechanically oriented bilayers (see Fig. 5b). Oriented bicelles are perfectly applicable to study transmembrane segments of proteins, though amphiphilic MAPs might interact with the rim and perturb the system in an unforeseen way. Lipidic nanodiscs, finally, fenced in, e.g. by an apolipoprotein belt, can in principle be used in the same way as magnetically oriented bicelles [90].

Lamellar bilayers formed from synthetic lipids are the preferred models that most closely mimic natural cell membranes. Vesicles – or liposomes – with distinct sizes and degrees of lamellarity (see Fig. 5) can be prepared by extrusion, dialysis, sonication, vortexing, freeze-thawing or similar treatments [91, 92]. In vigorously sonicated lipid dispersions [75–77, 93] the overall molecular re-orientation is relatively fast on the NMR time scale due to tumbling of the SUVs and/or lateral diffusion of the lipids around the curved surfaces. Such orientational averaging, however, can be essentially ignored in multilamellar vesicles, which are typically prepared as non-oriented samples for ssNMR with a total water content of about 50 wt%. In these samples the full spherical distribution of molecular orientations makes the above-mentioned anisotropic ssNMR approach theoretically possible though less straightforward in the case of mobile peptides, while being impossible in the case of immobilized peptides.

Compared to the sizes of living cells,[1] IUV and LUV resemble the dimensions of enveloped viruses (ranging from 80 to 400 nm) [94], while GUVs resemble typical bacteria and erythrocytes (1–7 μm). Eukaryotic cells tend to be even larger (10–30 μm in animals, 10–100 μm in plants). These dimensions imply that, except for viruses or specific sub-cellular membranes, flat bilayers are the only relevant membrane models. Hence, macroscopically oriented bilayers on solid supports (see

[1] http://bionumbers.hms.harvard.edu.

Figs. 2a and 5b) are a good choice for ssNMR structure analysis of MAPs [23, 47, 55]. The fact that mechanically aligned multi-bilayer stacks are hydrated close to 100% but do not contain any excess bulk water turns into an important but often overlooked advantage. Since the binding equilibrium of a peptide is driven completely towards the membrane-bound state under these conditions, even when electrostatics are not optimal, MAPs with a low membrane-affinity or in certain cases even transient states can also be trapped and characterized [95–97]. In mechanically supported bilayers the lipid composition can be chosen in a highly flexible way, the peptide concentration can be fully controlled, and it has even been possible to prepare pH-controlled samples recently. The physico-chemical aspects of peptide–lipid interactions are conveniently modelled in binary or ternary mixtures of synthetic phospholipids. For example, systems based on the uncharged 1,2-dimyristoyl-glycero-3-phosphocholine (DMPC, a good bilayer-forming lipid with a chain melting phase transition temperature around 22 °C, which is stable against oxidation, hydrolysis, etc.) can be combined with an anionic species such as 1,2-dimyristoyl-glycero-3-phosphoglycerol (DMPG, which mixes smoothly with DMPC without phase segregation), and/or with cholesterol (which modulates membrane fluidity in animals), and/or with 1-palmitoyl-2-oleoyl-glycero-3-phos phoethanolamine (POPE, which has an intrinsic negative curvature and favours inverted hexagonal phases), etc. Our two representative antimicrobial peptides PGLa and GS (Fig. 2) have been extensively studied by ^{19}F-NMR in supported membranes over a wide range of conditions by systematically varying the lipid composition, membrane charge, peptide concentration, lipid phase state, degree of sample hydration and spontaneous lipid curvature [33, 46, 65–67, 95–99]. These physico-chemical factors have been found to affect the peptide behaviour, as characterized in terms of molecular orientation, re-alignment and self-assembly, in a logical and comprehensive way.

The more biological properties of native membranes with highly complex lipid compositions can be imitated by choosing appropriate mixtures reflecting the major components of a typical prokaryotic or eukaryotic membrane [55, 97, 100, 101]. The lipid acyl chains tend to be partially unsaturated, rendering the bilayers in a liquid crystalline state, though various kinds of gel-like microdomains are known to co-exist. Prokaryotic membranes are conveniently modelled by mixtures of anionic phosphatidylglycerols (PG) and cardiolipins (CL) with zwitterionic phosphatidylethanolamines (PE) [102–104]. Eukaryotic plasma membranes, on the other hand, consist mainly of zwitterionic phosphatidylcholines (PC), sphingomyelines (SM) and PE. They also contain small but significant amounts of PG, phosphatidylserines (PS) and phosphatidylinositols (PI). One of the major differences to *prokaryotes* is the presence of cholesterol, which provides the *eukaryotes* with enhanced membrane stability. However, this is a highly oversimplified view, as there are thousands of lipid species present in every native membrane. The analysis and documentation of all membrane lipids from different types of cells is a project of global dimensions, and one of the main goals of the recent post-genome screening initiatives [105].

Given the overwhelming compositional complexity of biomembranes, a slightly better representation can be achieved when lipid extracts from native sources are used

for bilayer formation (e.g. the total or polar *E. coli* extracts, or preparations from bovine brain, liver or heart, which are all available commercially). The batch-to-batch reproducibility of individual preparations is limited, and a more serious problem is that these "total" extracts are prepared from the whole tissue. Hence they naturally contain some non-lipidic hydrophobic molecules, and in eukaryotic cases they do not originate from a single membrane type but contain all components from all membranous organelles as well. In these samples, due to their comparatively poor compositional characterization, it is difficult to specify a peptide-to-lipid ratio. Instead, weight/weight ratios can be used, or the number of phospholipid molecules can be estimated from phosphate determination, using, e.g. a Bartlett or Stewart assay [91, 106].

4 Native Biomembranes

Intact biological membranes are far more complex systems than even the lipid extracts (see Fig. 6). In hardly any case do the lipid components exceed 50% of the dry weight, as membranes intrinsically contain numerous proteins and various glycoconjugates. This diversity is most pronounced in the plasma membrane (irrespective of the genera) which is effectively amalgamated with the non-lipidic

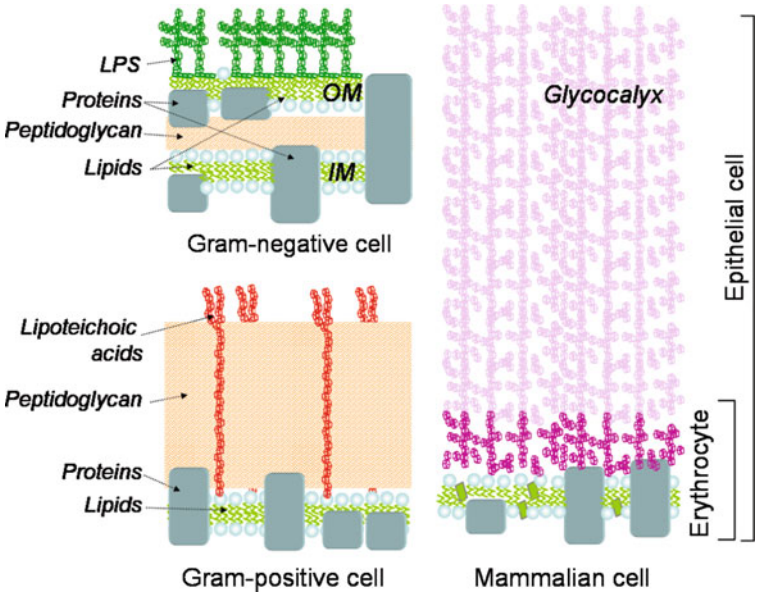

Fig. 6 Illustration of representative cell envelopes from *prokaryotes* and *eukaryotes* that are typically encountered by antimicrobial peptides. The key components of the biomembranes and cell wall or glycocalyx are shown, and the averaged protein content and typical dimensions are drawn to scale

exoskeleton or glycocalyx. Bacteria possess a rigid cell wall outside the cell membrane, which are together referred to as the cell envelope. The cell wall consists of the heteropolymer peptidoglycan, in which linear chains of alternating *N*-acetylglucosamine and *N*-acetylmureic acid are cross-linked by group- and strain specific, often unusual, amino acids [107, 108].

In Gram-positive species the cell wall is assembled from multiple layers to about 25 nm thickness, and it is covered by extracellular anionic polymers which contribute up to 10% of the total weight [109–111]. Typical are teichoic acids (TA), which are phosphorus-containing polymers with 16 to 40 units of ribitol or glycerol that can be adenylated and/or glycosylated. TAs are either covalently bound to the peptidoglycan (wall teichoic acids – WTA) or anchored in the membrane via a glycolipid (lipoteichoic acids – LTA). A few Gram-positive bacteria do not possess conventional LTA and WTA, but instead have functionally analogous polyanions. *Micrococcus luteus*, for instance, possesses lipomannan, a polymer of mannosyl residues being esterified with succinyl groups to approximately 25% [110, 112, 113].

In Gram-negative bacteria the cell wall is only about 3 nm thick, and located in the extended periplasmatic space between the inner membrane (IM) and an additional outer membrane (OM). The lipid monolayer in the outer leaflet of the OM contains about 90% lipopolysaccharides (LPS). LPS consist of Lipid A and an oligosaccharide component, which is highly specific for individual bacterial species and phenotypes [108, 114].

Unlike other *Eukarya*, animal cells lack cell walls, though they tend to be surrounded by a highly developed glycocalyx of up to 140 nm in thickness [108]. This diffuse layer of densely packed oligosaccharides has a heterogeneous composition and is connected to the membrane via lipids or integral proteins. The "boundary" of the cell usually extends beyond the mere lipid bilayer with its embedded proteins, and the extracellular structures provide initial sites of interaction or are themselves targets for MAPs such as antimicrobial peptides [115].

4.1 Erythrocyte Ghosts

Erythrocytes are probably the best-established cell system and the most common model for eukaryotic cell membranes. For instance, in evaluations of MAPs as antibiotics, their cytolytic effect on red blood cells is routinely studied in haemolysis assays as a general measure of toxic side-effects [116, 117]. In human erythrocytes, which do not contain a nucleus or intracellular organelles, the protein-to-lipid ratio is about 1:1 (wt/wt). Of the membrane lipids, 60–80% are phospholipids (SM and PC in the outer monolayer; PE, PS and PI in the inner one), up to 25% cholesterol, and up to 10% glycolipids. The latter are almost entirely (95%) located in the outer leaflet [103, 118, 119]. To prepare erythrocyte membranes as so-called "ghosts", the cells are exposed in extensive washing steps to a hypotonic medium, which causes them to swell and the membrane permeability to increase. The membrane reseals again for larger molecules like haemoglobin, but stays

permeable for smaller compounds like ions [119–121]. By repeated washing/centrifugation cycles the cytoplasm is effectively removed, and upon membrane re-sealing "ready-to-use" ghost suspensions are obtained [122–124]. These are accessible relatively quickly (in a couple of days), in large quantities (several tens of milligrams from a single blood bag) and low in contaminations [122, 125].

Several ssNMR investigations have already been performed on erythrocyte membrane vesicles [126, 127] and even on erythrocyte membranes oriented by an isopotential spin-dry ultracentrifugation technique [128]. However, this latter procedure is rather tedious and not really required, as we recently found that orientation can also be achieved by depositing a ghost suspension onto a glass slide, followed by vapour-phase equilibration against a saturated K_2SO_4 solution (96% humidity [129]) [124]. Representative solid-state ^{31}P-NMR spectra of non-oriented and of macroscopically aligned ghosts prepared this way are shown in Fig. 7. The non-oriented membranes yield classical "powder" lineshapes with the characteristic dimensions (CSA span of ~ 35 ppm) of synthetic phospholipid bilayers [124, 128]. The spectra of the oriented ghost samples are also equivalent to those of model phospholipid bilayers. At the horizontal sample alignment they show a narrow lipid signal (6–7 ppm width), which is scaled by the factor −1/2 after tilting the sample to 90° in the static magnetic field [124]. Notably, no separate signals of individual types of phospholipids in erythrocyte membranes are resolved. A small isotropic component of varying intensity was observed in different freshly prepared samples and can be attributed to residual inorganic phosphorus after washing, or to a small fraction of lipidic non-bilayer phases

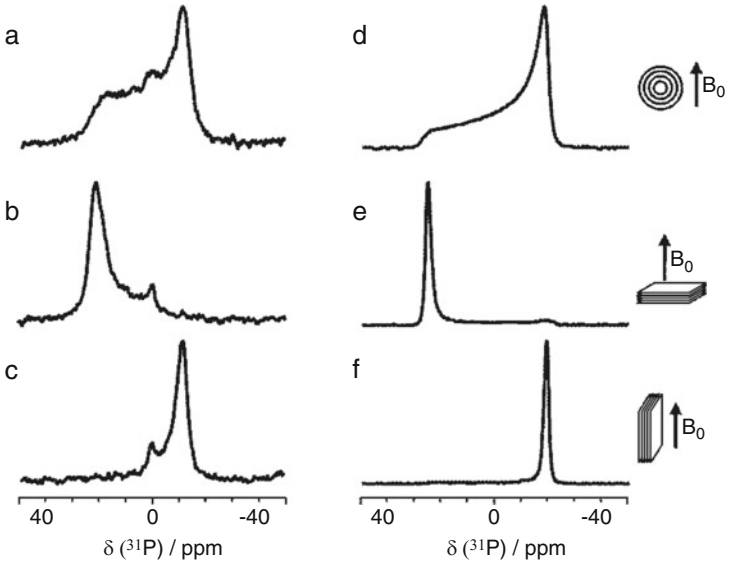

Fig. 7 Comparison of the solid-state ^{31}P-NMR spectra from erythrocyte ghosts (*left column*) and of DMPC model membranes (*right column*). Samples are prepared as a non-oriented suspension in excess water (**a**, **d**), and as macroscopically oriented membranes on glass slides that are aligned either parallel (**b**, **e**) or perpendicular (**c**, **f**) to the static magnetic field

like micelles or a cubic phase. Nevertheless, these isotropic signals were found to be useful as an internal reference and as an indicator on the hydration status. They are sharp in freshly prepared samples, but broaden, decrease or vanish during long NMR measurements or upon heating, due to drying of the sample, since the intensity is restored after rehydration in a humid atmosphere.

When the ^{19}F-labelled antimicrobial peptide PGLa was co-incubated with ghosts in the final washing step, the ^{19}F-NMR signal was fully contained in the pellet after centrifugation, which indicates complete membrane binding [124]. The corresponding ^{31}P-NMR spectra showed no difference between peptide-supplemented and peptide-free preparations up to a peptide-to-lipid ratio of P/L $\approx$ 1:20 (mol/mol) (as estimated by a modified Bartlett phosphorus assay [91]). By analyzing the same four ^{19}F-labelled PGLa analogues as in the model membrane studies cited above, we found that this α-helical peptide assumes a surface-aligned state in ghost membranes. It could thus be demonstrated for the first time that the sensitivity of ^{19}F-NMR and the lack of a natural abundance background indeed permit ssNMR studies of native biomembranes. The lineshapes were broader and less well resolved than in model membranes, and NMR measuring times were up to 36 h (compared to 12 h for the same P/L $\approx$ 1:300 in DMPC/DMPG). Nevertheless, a comparison of the characteristic dipolar splittings provided a unique answer on the dominant alignment state of PGLa in ghost membranes. We did not, however, find evidence for a tilted or membrane-inserted state of the peptide that would correspond to the formation of a transmembrane pore, as had been detected in DMPC model membranes [96, 130]. In contrast to the more uniform situation in synthetic lipids, where unique alignment states could be trapped, it was noted that multiple peptide pools co-exist in the ghost samples. A significant proportion of the spectral intensity corresponded to an immobilized and non-oriented "powder" fraction of peptides. This signal got reduced with increasing temperature and was attributed to peptides bound to the glycocalyx rather than the lipid bilayer [124].

More recently we observed a similar picture for the ^{19}F-labelled antimicrobial peptide gramicidin S in ghost membranes, which is illustrated in Fig. 8 and has not been published before. At low temperature the ^{19}F-NMR signal of ^{19}F-labelled GS is very broad (Fig. 8c) and corresponds to the "powder" lineshape that is known from DMPC/cholesterol model membranes (Fig. 8f). Under these conditions the peptide is immobilized and not bound to the membranes in any well-defined, oriented manner [130]. Upon raising the temperature, a narrow signal successively appears close to −117 ppm (Fig. 8a, d), which can be assigned to surface-aligned peptides [65, 96]. At around 25 °C in DMPC bilayers, an additional broad signal appears transiently near −80 ppm (Fig. 8e), which has been attributed to peptide molecules that have flipped their alignment and inserted into the membrane as a putative oligomeric pore [96, 97, 130]. In ghost membranes, we have carefully analyzed the corresponding region of the spectrum to obtain evidence for such an upright peptide orientation. However, spectral the intensity seen around 35 °C in ghosts (Fig. 8b) is only a remnant of the powder contribution and does not signify an inserted alignment of the peptide as a pore.

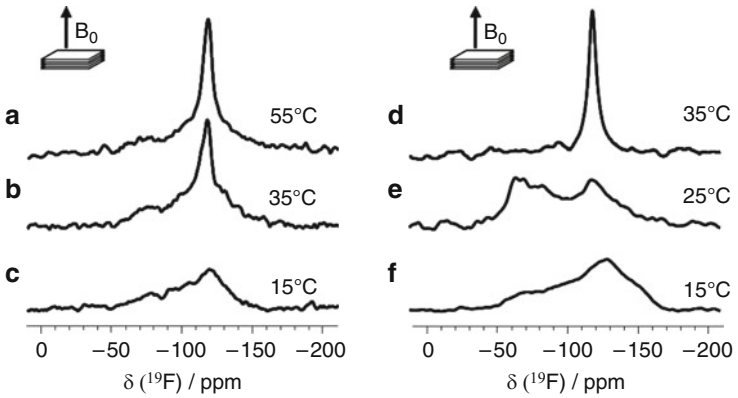

Fig. 8 Representative solid-state ^{19}F-NMR spectra of ^{19}F-labelled gramicidin S (substituted at both Leu positions with 4F-Phg), embedded in macroscopically oriented ghost membranes (*left column*) and DMPC bilayers (*right column*) at a peptide-to-lipid ratio of about 1:40 [in (F) the lipid was 1:1 DMPC/cholesterol]. Depending on temperature, the peptide can assume different alignment states, which are strikingly similar in the native membranes and the model bilayers

In summary, we may thus conclude that PGLa and GS do not form stable, NMR-observable pores in native membrane as readily as they do in model bilayers. The corresponding tilted and/or inserted states of our two representative MAPs could only be comprehensively characterized in DMPC-based samples, where the peptides could be trapped in a uniform state. In living cells, on the other hand, these states would seem to be only of a transient nature, i.e. at the very moment when the antimicrobial peptide attacks the membrane and passes through the lipid barrier along its concentration gradient towards the cytosol.

4.2 Bacterial Protoplasts

As for erythrocyte ghosts and other animal cell membranes, protocols for bacterial membrane isolation have been used for decades by cell microbiologists [131]. Until our pioneering ^{19}F-NMR study on PGLa in native membranes [124], however, such preparations were not employed in ssNMR spectroscopy. Initial attempts to copy the alignment procedure for ghosts with Gram-positive *Bacillus subtilis* protoplasts had failed at the stage of obtaining "clean" ^{31}P-NMR spectra, as they were dominated by an intense isotropic signal. Since this component could not be removed by extensive washing, it was obviously membrane-bound and originated from TA, which are known to be abundant in the envelope of most Gram-positive bacteria including *B. subtilis*. Even bacteria that are devoid of TA often still possess phosphate-containing anionic cell wall components, like lipomannanes [109, 110]. Lipomannan of *Micrococci*, however, is a lucky exception as it completely lacks phosphates [132], and *M. luteus* is a typical example of these microorganisms.

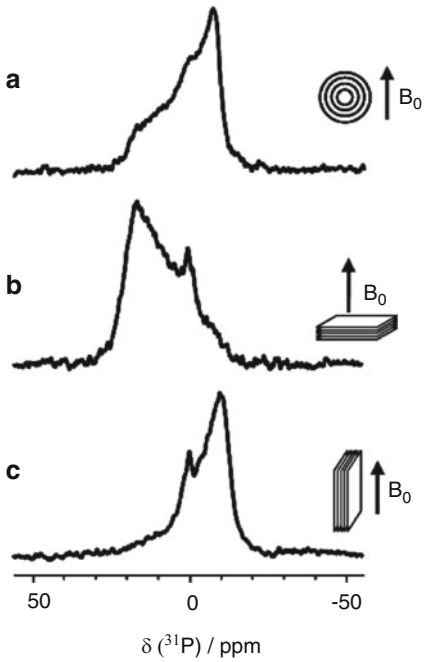

Fig. 9 Representative solid-state ^{31}P-NMR spectra from *M. luteus* protoplasts, prepared as a non-oriented suspension in excess water (**a**), and as macroscopically oriented membranes on glass slides that are aligned either parallel (**b**) or perpendicular (**c**) to the static magnetic field

The ratio of protein to lipid in the cell membrane of *M. luteus* is about 7 to 3 (wt/wt), and the lipids comprise up to 70% negatively charged PG. This lipid is predominantly located in the outer monolayer, and the remaining 30% dimannosyldiacylglycerol (DMDG) are symmetrically distributed between both leaflets [103, 133].

To prepare native membranes from *M. luteus* by osmotic lysis in a similar manner as described for erythrocytes, the thick cell wall first needs to be removed by lysozyme, and the protoplasts can be treated with hypotonic medium [122, 123]. Similar to erythrocyte ghosts, *M. luteus* protoplast preparations can be aligned on glass slides, as seen in Fig. 9. Once again, no separate ^{31}P-NMR signals of individual types of phospholipids are resolved, and isotropic signals with low intensity are present, within a CSA span of about 27 ppm. However, the linewidths of the oriented protoplast membranes are significantly larger than in oriented ghosts. This higher mosaic spread might be a consequence of the higher percentage of proteins in membranes of *M. luteus*. On top of that, the surface area of a flattened bacterial protoplasts ($\leq$ 12 μm^2) is more than an order of magnitude smaller than that of an erythrocyte ($\geq$ 120 μm^2), with a correspondingly higher number of edge defects in an oriented sample (see Fig. 2d). Together with the fast diffusion of lipids around these highly curved defects, this will contribute a broadening of the oriented signals within a narrowed CSA span.

In these protoplast preparations the possibility of solid-state ^{19}F-NMR was also demonstrated using PGLa, and the presence of a surface-bound α-helix was

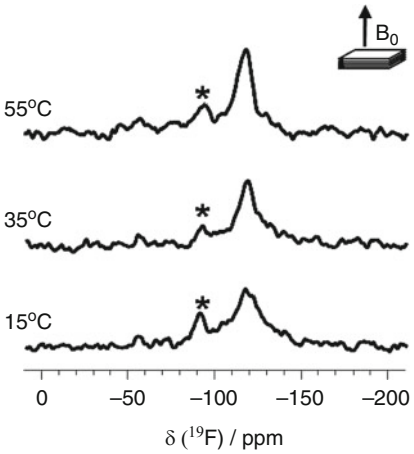

Fig. 10 Representative solid-state ^{19}F-NMR spectra of ^{19}F-labelled gramicidin S (substituted at both Leu positions with 4F-Phg), embedded in macroscopically oriented bacterial protoplasts at a peptide-to-lipid ratio of about 1:40. These membrane samples are intrinsically less well oriented than the ghosts in Fig. 8, and a TFA contamination is marked with an *asterisk*

confirmed [124]. Our more recent spectra of ^{19}F-labelled GS (Fig. 10) support a similar surface-bound state at higher temperature, and a more immobilized fraction at low temperature, similar to the situation seen in ghost membranes (Fig. 8). These data are less clear-cut, however, and also of a lower quality. While it had been noted that the protoplasts of *M. luteus* bind about tenfold more PGLa than erythrocyte ghosts, this could not be confirmed for GS.

4.3 LPS-Containing Membranes

Having established a suitable system to study MAPs in native membranes from Gram-positive bacteria, it would also be very interesting to characterize their interactions with Gram-negative ones. An antimicrobial peptide will at first encounter the LPS-monolayer of the OM, which we have accordingly tried to prepare as an oriented NMR sample. The hope was to use so-called exosomes as intrinsic membrane sources, as these vesicles (MV) are constitutively secreted by almost any cell type [134–136]. In common animal cells there are only a few dozen exosomes per cell and the accessible amount of material precludes mass production, but for bacteria the situation is advantageous [137, 138]. Like many other biofilms producing Gram-negative bacteria, *Pseudomonas aeruginosa*, for instance, is able to produce MVs in milligram quantities per litre. As these MVs have budded off from the OM of the cell envelope, they constitute a genuine, asymmetrical LPS-lipid bilayer. They are 50–100 nm in diameter and provide communication between cells, defence against harmful substances, or mediate toxicity towards the host organism. Following a period of bacterial growth, the MVs can be obtained from

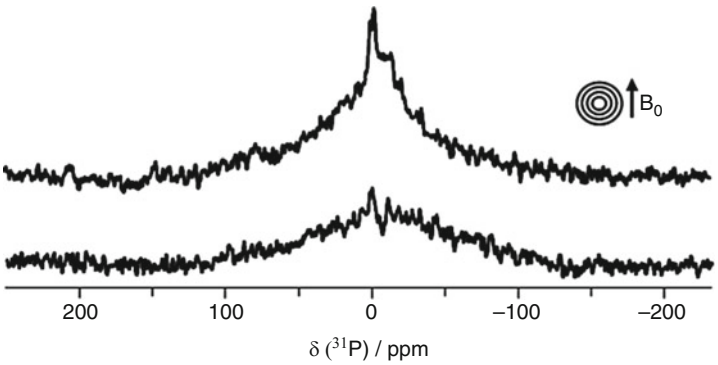

Fig. 11 Representative ^{31}P-ssNMR spectra from exosomes of *P. aeruginosa* prepared as suspensions in water excess. Preparations are from two strains, which differ in their LPS structure: rmlC (*top*) and PAO1 (*bottom*). Spectra are dominated by signals from DNA

a cell-free supernatant by ultracentrifugation [139–141]. In contrast to the erythrocyte ghosts and protoplasts of *M. luteus*, however, we have not found the harvested MVs to be applicable for ssNMR. The ^{31}P-NMR spectra are much broader and dominated by an isotropic component, as illustrated in Fig. 11. Detected significant amounts of DNA in these preparations interfere with the ^{31}P-NMR, which emphasises that the interior of MV should not be ignored. Yet, by optimized washing procedures and with application of nucleases, some control over these might be gained. Furthermore, the very small size of these vesicles makes the prospect of obtaining well-oriented membrane samples rather gloomy, given our experience with the increased abundance of defects in the oriented protoplast samples compared to the ghosts.

5 Limitations and Future Perspectives

On the way towards *in-cell* NMR, the principle feasibility of studying MAPs in native cell membranes by solid-state ^{19}F-NMR has now been demonstrated for two examples: the antimicrobial peptides PGLa and gramicidin S. Further applications can now be envisaged for other MAPs with simple secondary structures like short temporins [142], magainins [143], and designer-made analogues like MSI-103 [144], MAP [145], or BP100 [146], which are currently being characterized in lipid model membranes. In parallel, other types of cell membranes could be explored, from plants, fungi, and even from intracellular organelles. From the methodological perspective, the main restrictions are (a) the absence of ^{31}P-signals other than from phospholipids to allow a characterization of the oriented membranes, and (b) the membrane preparation should yield sufficient material (several milligrams of dry weight per sample).

The solid-state ^{19}F-NMR experiments have become possible by exploiting the high sensitivity of fluorine and its lack of a natural abundance background on the one hand, and by optimizing the preparation of oriented samples from native membranes on the other. These two aspects also represent the critical points for further improvements in moving from native membranes towards living cells. The whole arsenal of signal enhancement approaches could be applied by using novel hardware, DNP, and/or ^{19}F-NMR. Sufficient sensitivity and signal-to-noise would even alleviate the need to prepare macroscopically aligned samples when working with small, rapidly diffusing peptides in fluid membranes.

In these first demonstration studies we have always found the peptides to be in a structurally more heterogeneous situation than in model bilayers, as evident from the multi-component ^{19}F-NMR spectra. There were multiple peptide fractions co-existing in these samples, including not only surface-bound but also immobilized and freely tumbling peptide pools. Their relative proportions varied with temperature, but no conditions could be found where a single species was uniformly present. This finding is not surprising, given that extra-membranous carbohydrate- and protein-rich layers are present in native membranes, with dimensions similar to or larger than the lipid bilayer. Essentially, due to this complexity of biological membranes, the *in-cell* NMR determination of structural parameters for any MAP is *de facto* going to be intrinsically difficult. It has so far not been possible to detect a tilted or membrane-inserted state of a ^{19}F-labelled peptide in a native membrane sample, which has been reported from model membrane studies to represent distinct re-alignment steps into a transmembrane pore. This lack of data may have two reasons: (a) either the experimental conditions have not yet been found to trap these remarkable alignment states, and/or (b) the pore-associated state may occur only transiently and/or only at very low concentration in the heterogeneous environment of a native cell membrane. Nevertheless, having demonstrated here the fundamental similarity of a peptide's alignment in model bilayers and in native membranes, it is straightforward now to screen the structural behaviour and orientational states of MAPs in model membranes before further characterizing a selected few in native biomembranes. Especially the comparison between bacterial protoplasts and eukaryotic ghost membranes, including quantitative binding affinities and stepwise re-alignment thresholds by NMR, should help to shed light on the selectivity of antimicrobial peptides in terms of their molecular mechanisms of membrane perturbation.

Acknowledgements We thank PEPSY-lab at IBG2 for peptide material, and the DFG-Center for Functional Nanostructures (TP E1.2) for supporting the NMR facility.

References

1. Serber Z, Selenko P, Hansel R, Reckel S, Lohr F, Ferrell JE, Wagner G, Dotsch V (2006) Investigating macromolecules inside cultured and injected cells by in-cell NMR spectroscopy. Nat Protoc 1:2701–2709

2. Burz DS, Dutta K, Cowburn D, Shekhtman A (2006) Mapping structural interactions using in-cell NMR spectroscopy (STINT-NMR). Nat Methods 3:91–93
3. Burz DS, Shekhtman A (2008) In-cell biochemistry using NMR spectroscopy. PLoS One 3: e2571
4. Sakakibara D, Sasaki A, Ikeya T, Hamatsu J, Hanashima T, Mishima M, Yoshimasu M, Hayashi N, Mikawa T, Walchli M, Smith BO, Shirakawa M, Guntert P, Ito Y (2009) Protein structure determination in living cells by in-cell NMR spectroscopy. Nature 458:102–105
5. Reckel S, Hansel R, Lohr F, Dotsch V (2007) In-cell NMR spectroscopy. Prog Nucl Magn Reson Spectrosc 51:91–101
6. McNeill SA, Gor'kov PL, Shetty K, Brey WW, Long JR (2009) A low-E magic angle spinning probe for biological solid state NMR at 750 MHz. J Magn Reson 197:135–144
7. Dvinskikh SV, Castro V, Sandstrom D (2004) Heating caused by radiofrequency irradiation and sample rotation in C-13 magic angle spinning NMR studies of lipid membranes. Magn Reson Chem 42:875–881
8. Griffin RG, Prisner TF (2010) High field dynamic nuclear polarization-the renaissance. Phys Chem Chem Phys 12:5737–5740
9. Selenko P, Wagner G (2007) Looking into live cells with in-cell NMR spectroscopy. J Struct Biol 158:244–253
10. Reckel S, Lohr F, Dotsch V (2005) In-cell NMR spectroscopy. ChemBioChem 6:1601–1606
11. Bhattacharya A (2009) Protein structures: structures of desire. Nature 459:24–27
12. Brown FF, Campbell ID, Kuchel PW, Rabenstein DC (1977) Human erythrocyte metabolism studies by H-1 spin-echo NMR. FEBS Lett 82:12–16
13. Pielak GJ, Li CG, Miklos AC, Schlesinger AP, Slade KM, Wang GF, Zigoneanu IG (2009) Protein nuclear magnetic resonance under physiological conditions. Biochemistry-US 48:226, 9170
14. Inomata K, Ohno A, Tochio H, Isogai S, Tenno T, Nakase I, Takeuchi T, Futaki S, Ito Y, Hiroaki H, Shirakawa M (2009) High-resolution multi-dimensional NMR spectroscopy of proteins in human cells. Nature 458:106–109
15. Hu KN, Tycko R (2010) What can solid state NMR contribute to our understanding of protein folding? Biophys Chem 151:10–21
16. Bockmann A, Meier BH (2010) Prions en route from structural models to structures. Prion 4:72–79
17. Brown MF, Salgado GFJ, Struts AV (2010) Retinal dynamics during light activation of rhodopsin revealed by solid-state NMR spectroscopy. BBA-Biomembranes 1798:177–193
18. Tompa P (2009) Structural disorder in amyloid fibrils: its implication in dynamic interactions of proteins. FEBS J 276:5406–5415
19. Ramamoorthy A (2009) Beyond NMR spectra of antimicrobial peptides: dynamical images at atomic resolution and functional insights. Solid State Nucl Mag 35:201–207
20. Baldus M (2007) Magnetic resonance in the solid state: applications to protein folding, amyloid fibrils and membrane proteins. Eur Biophys J 36(Suppl 1):S37–48
21. Opella SJ, Nevzorov A, Mesleb MF, Marassi FM (2002) Structure determination of membrane proteins by NMR spectroscopy. Biochem Cell Biol 80:597–604
22. Afonin S, Juretic D, Separovic F, Ulrich AS (2011) Special issue on membrane-active peptides. Eur Biophys J 40:347–348
23. Naito A (2009) Structure elucidation of membrane-associated peptides and proteins in oriented bilayers by solid-state NMR spectroscopy. Solid State Nucl Mag 36:67–76
24. Hong M (2006) Oligomeric structure, dynamics, and orientation of membrane proteins from solid-state NMR. Structure 14:1731–1740
25. Hong M (2007) Structure, topology, and dynamics of membrane peptides and proteins from solid-state NMR spectroscopy. J Phys Chem B 111:10340–10351
26. Zelezetsky I, Tossi A (2006) Alpha-helical antimicrobial peptides – using a sequence template to guide structure–activity relationship studies. BBA-Biomembranes 1758:1436–1449

27. Scott RW, DeGrado WF, Tew GN (2008) De novo designed synthetic mimics of antimicrobial peptides. Curr Opin Biotechnol 19:620–627
28. Epand RM, Vogel HJ (1999) Diversity of antimicrobial peptides and their mechanisms of action. BBA-Biomembranes 1462:11–28
29. Giuliani A, Pirri G, Bozzi A, Di Giulio A, Aschi M, Rinaldi AC (2008) Antimicrobial peptides: natural templates for synthetic membrane-active compounds. Cell Mol Life Sci 65:2450–2460
30. Danielson MA, Falke JJ (1996) Use of F-19 NMR to probe protein structure and conformational changes. Annu Rev Biophys Biomol Struct 25:163–195
31. Yu JX, Kodibagkar VD, Cui WN, Mason RP (2005) F-19: a versatile reporter for noninvasive physiology and pharmacology using magnetic resonance. Curr Med Chem 12:819–848
32. Ulrich AS (1999) High resolution solid state NMR, 1H, 19F. In: Lindon J, Tranter G, Holmes J (eds) Encyclopedia of spectroscopy and spectrometry. Elsevier, Oxford, pp 813–825
33. Strandberg E, Wadhwani P, Tremouilhac P, Durr UHN, Ulrich AS (2006) Solid-state NMR analysis of the PGLa peptide orientation in DMPC bilayers: structural fidelity of H-2-labels versus high sensitivity of F-19-NMR. Biophys J 90:1676–1686
34. Glaser RW, Ulrich AS (2003) Susceptibility corrections in solid-state NMR experiments with oriented membrane samples. Part I: applications. J Magn Reson 164:104–114
35. Wadhwani P, Strandberg E (2009) Structure analysis of membrane-active peptides using 19F-labeled amino acids and solid-state NMR. In: Ojima I (ed) Fluorine in medicinal chemistry and chemical biology. Wiley, Chichester, pp 463–493
36. Wadhwani P, Tremouilhac P, Strandberg E, Afonin S, Grage S, Ieronimo M, Berditsch M, Ulrich AS (2007) Using fluorinated amino acids for structure analysis of membrane-active peptides by solid-state 19F-NMR. In: Soloshonok V, Mikami K, Yamazaki T, Welch JT, Honek J (eds) Current fluoroorganic chemistry (ACS symposium series). American Chemical Society, Washington, pp 431–446
37. Ulrich AS (2005) Solid state F-19 NMR methods for studying biomembranes. Prog Nucl Magn Reson Spectrosc 46:1–21
38. Mason RP (1999) Transmembrane pH gradients in vivo: measurements using fluorinated vitamin B6 derivatives. Curr Med Chem 6:481–499
39. Brindle K, Williams S-P, Boulton M (1989) 19F NMR detection of a fluorine-labelled enzyme in vivo. FEBS Lett 255:121–124
40. Li CG, Wang GF, Wang YQ, Creager-Allen R, Lutz EA, Scronce H, Slade KM, Ruf RAS, Mehl RA, Pielak GJ (2010) Protein F-19 NMR in *Escherichia coli*. J Am Chem Soc 132:321–327
41. Gor'kov PL, Witter R, Chekmenev EY, Nozirov F, Fu R, Brey WW (2007) Low-E probe for F-19-H-1 NMR of dilute biological solids. J Magn Reson 189:182–189
42. Haase J, Curro NJ, Slichter CP (1998) Double resonance probes for close frequencies. J Magn Reson 135:273–279
43. Graether SP, DeVries JS, McDonald R, Rakovszky ML, Sykes BD (2006) A H-1/F-19 minicoil NMR probe for solid-state NMR: application to 5-fluoroindoles. J Magn Reson 178:65–71
44. Andrushchenko VV, Vogel HJ, Prenner EJ (2007) Optimization of the hydrochloric acid concentration used for trifluoroacetate removal from synthetic peptides. J Pept Sci 13:37–43
45. Valenti LE, Paci MB, De Pauli CP, Giacomelli CE (2011) Infrared study of trifluoroacetic acid unpurified synthetic peptides in aqueous solution: trifluoroacetic acid removal and band assignment. Anal Biochem 410:118–123
46. Glaser RW, Sachse C, Durr UHN, Wadhwani P, Ulrich AS (2004) Orientation of the antimicrobial peptide PGLa in lipid membranes determined from F-19-NMR dipolar couplings of 4-CF3-phenylglycine labels. J Magn Reson 168:153–163
47. Park SH, Das BB, De Angelis AA, Scrima M, Opella SJ (2010) Mechanically, magnetically, and "rotationally aligned" membrane proteins in phospholipid bilayers give equivalent angular constraints for NMR structure determination. J Phys Chem B 114:13995–14003

48. Strandberg E, Ulrich AS (2004) NMR methods for studying membrane-active antimicrobial peptides. Concepts Magn Reson A 23A:89–120
49. Strandberg E, Esteban-Martin S, Salgado J, Ulrich AS (2009) Orientation and dynamics of peptides in membranes calculated from 2H-NMR data. Biophys J 96:3223–3232
50. Esteban-Martin S, Strandberg E, Salgado J, Ulrich AS (2010) Solid state NMR analysis of peptides in membranes: influence of dynamics and labeling scheme. BBA-biomembranes 1798:252–257
51. Esteban-Martin S, Strandberg E, Fuertes G, Ulrich AS, Salgado J (2009) Influence of whole-body dynamics on 15N PISEMA NMR spectra of membrane proteins: a theoretical analysis. Biophys J 96:3233–3241
52. Afonin S, Dur UHN, Glaser RW, Ulrich AS (2004) 'Boomerang'-like insertion of a fusogenic peptide in a lipid membrane revealed by solid-state F-19 NMR. Magn Reson Chem 42:195–203
53. Mykhailiuk PK, Afonin S, Palamarchuk GV, Shishkin OV, Ulrich AS, Komarov IV (2008) Synthesis of trifluoromethyl-substituted proline analogues as F-19 NMR labels for peptides in the polyproline II conformation. Angew Chem Int Edit 47:5765–5767
54. Grasnick D, Sternberg U, Strandberg E, Wadhwani P, Ulrich AS (2011) Irregular structure of the HIV fusion peptide in membranes demonstrated by solid-state NMR and MD simulations Eur Biophys J 40:529–543
55. Auger M (2000) Biological membrane structure by solid-state NMR. Curr Issues Mol Biol 2:119–124
56. Rainey JK, Sykes BD (2005) Optimizing oriented planar-supported lipid samples for solid-state protein NMR. Biophys J 89:2792–2805
57. Aisenbrey C, Bertani P, Bechinger B (2010) Solid-state NMR investigations of membrane-associated antimicrobial peptides. Methods Mol Biol 618:209–233
58. Young TS, Schultz PG (2010) Beyond the canonical 20 amino acids: expanding the genetic lexicon. J Biol Chem 285:11039–11044
59. Jones DH, Cellitti SE, Hao X, Zhang Q, Jahnz M, Summerer D, Schultz PG, Uno T, Geierstanger BH (2010) Site-specific labeling of proteins with NMR-active unnatural amino acids. J Biomol NMR 46:89–100
60. Staunton D, Schlinkert R, Zanetti G, Colebrook SA, Campbell LD (2006) Cell-free expression and selective isotope labelling in protein NMR. Magn Reson Chem 44:S2–9
61. Kubyshkin VS, Komarov IV, Afonin S, Mykhailiuk PK, Grage SL, Ulrich AS (2011) Trifluoromethyl-substituted α-amino acids as solid state 19F-NMR labels for structural studies of membrane-bound peptides. In: Gouverneur V, Müller K (eds) Fluorine in pharmaceutical and medicinal chemistry: from biophysical aspects to clinical applications. Imperial College Press (in press)
62. Wadhwani P, Afonin S, Ieromino M, Buerck J, Ulrich AS (2006) Optimized protocol for synthesis of cyclic gramicidin S: starting amino acid is key to high yield. J Org Chem 71:55–61
63. Fields GB, Noble RL (1990) Solid-phase peptide-synthesis utilizing 9-fluorenylmethoxycarbonyl amino-acids. Int J Pept Prot Res 35:161–214
64. Mikhailiuk PK, Afonin S, Chernega AN, Rusanov EB, Platonov MO, Dubinina GG, Berditsch M, UIrich AS, Komarov IV (2006) Conformationally rigid trifluoromethyl-substituted alpha-amino acid designed for peptide structure analysis by solid-state F-19 NMR spectroscopy. Angew Chem Int Edit 45:5659–5661
65. Salgado J, Grage SL, Kondejewski LH, Hodges RS, McElhaney RN, Ulrich AS (2001) Membrane-bound structure and alignment of the antimicrobial beta-sheet peptide gramicidin S derived from angular and distance constraints by solid state F-19-NMR. J Biomol NMR 21:191–208
66. Afonin S, Glaser RW, Berditchevskaia M, Wadhwani P, Guhrs KH, Mollmann U, Perner A, Ulrich AS (2003) 4-Fluorophenylglycine as a label for F-19 NMR structure analysis of membrane-associated peptides. ChemBioChem 4:1151–1163

67. Afonin S, Mikhailiuk PK, Komarov IV, Ulrich AS (2007) Evaluating the amino acid CF3-bicyclopentylglycine as a new label for solid-state F-19-NMR structure analysis of membrane-bound peptides. J Pept Sci 13:614–623
68. Mink C (2009) Zusammenhänge von Struktur und Funktion unterschiedlicher membranaktiver Peptide. PhD thesis, University of Karlsruhe (KIT)
69. Tiltak D (2009) Strukturelle und funktionelle Untersuchungen der antimikrobiellen Peptide MSI- 103 und Temporin A. PhD thesis, University of Karlsruhe (KIT)
70. Maisch D, Wadhwani P, Afonin S, Bottcher C, Koksch B, Ulrich AS (2009) Chemical labeling strategy with (R)- and (S)-trifluoromethylalanine for solid state 19F NMR analysis of peptaibols in membranes. J Am Chem Soc 131:15596–15597
71. Pervushin KV, Orekhov V, Popov AI, Musina L, Arseniev AS (1994) Three-dimensional structure of (1–71)bacterioopsin solubilized in methanol/chloroform and SDS micelles determined by 15N-1H heteronuclear NMR spectroscopy. Eur J Biochem 219:571–583
72. Tyukhtenko S, Tiburu EK, Deshmukh L, Vinogradova O, Janero DR, Makriyannis A (2009) NMR solution structure of human cannabinoid receptor-1 helix 7/8 peptide: candidate electrostatic interactions and microdomain formation. Biochem Biophys Res Commun 390:441–446
73. Luca S, White JF, Sohal AK, Filippov DV, van Boom JH, Grisshammer R, Baldus M (2003) The conformation of neurotensin bound to its G protein-coupled receptor. Proc Natl Acad Sci USA 100:10706–10711
74. Lopez JJ, Shukla AK, Reinhart C, Schwalbe H, Michel H, Glaubitz C (2008) The structure of the neuropeptide bradykinin bound to the human G-protein coupled receptor bradykinin B2 as determined by solid-state NMR spectroscopy. Angew Chem Int Ed Engl 47:1668–1671
75. Sanders CR, Sonnichsen F (2006) Solution NMR of membrane proteins: practice and challenges. Magn Reson Chem 44 Spec No:S24–40
76. Henry GD, Sykes BD (1994) Methods to study membrane protein structure in solution. Methods Enzymol 239:515–535
77. Fernandez C, Wuthrich K (2003) NMR solution structure determination of membrane proteins reconstituted in detergent micelles. FEBS Lett 555:144–150
78. Sanders CR, Hare BJ, Howard KP, Prestegard JH (1994) Magnetically-oriented phospholipid micelles as a tool for the study of membrane-associated molecules. Prog Nucl Magn Reson Spectrosc 26:421–444
79. Marcotte I, Auger M (2005) Bicelles as model membranes for solid- and solution-state NMR studies of membrane peptides and proteins. Concept Magn Reson A 24A:17–37
80. Matsumori N, Murata M (2010) 3D structures of membrane-associated small molecules as determined in isotropic bicelles. Nat Prod Rep 27:1480–1492
81. Vold RR, Prosser RS, Deese AJ (1997) Isotropic solutions of phospholipid bicelles: a new membrane mimetic for high-resolution NMR studies of polypeptides. J Biomol NMR 9:329–335
82. Canlas CG, Ma D, Tang P, Xu Y (2008) Residual dipolar coupling measurements of transmembrane proteins using aligned low-q bicelles and high-resolution magic angle spinning NMR spectroscopy. J Am Chem Soc 130:13294–13300
83. Cross TA, Sharma M, Yi M, Zhou HX (2011) Influence of solubilizing environments on membrane protein structures. Trends Biochem Sci 36:117–125
84. Wang G (2008) NMR of membrane-associated peptides and proteins. Curr Protein Pept Sci 9:50–69
85. Bader R, Lerch M, Zerbe O (2003) NMR of membrane-associated peptides and proteins. In: Zerbe O (ed) BioNMR in drug research. Wiley-VCH, Weinheim, pp 95–120
86. Diller A, Loudet C, Aussenac F, Raffard G, Fournier S, Laguerre M, Grelard A, Opella SJ, Marassi FM, Dufourc EJ (2009) Bicelles: a natural 'molecular goniometer' for structural, dynamical and topological studies of molecules in membranes. Biochimie 91:744–751
87. Nieh MP, Raghunathan VA, Glinka CJ, Harroun TA, Pabst G, Katsaras J (2004) Magnetically alignable phase of phospholipid "bicelle" mixtures is a chiral nematic made up of wormlike micelles. Langmuir 20:7893–7897

88. van Dam L, Karlsson G, Edwards K (2006) Morphology of magnetically aligning DMPC/DHPC aggregates-perforated sheets, not disks. Langmuir 22:3280–3285
89. Prosser RS, Hwang JS, Vold RR (1998) Magnetically aligned phospholipid bilayers with positive ordering: a new model membrane system. Biophys J 74:2405–2418
90. Borch J, Hamann T (2009) The nanodisc: a novel tool for membrane protein studies. Biol Chem 390:805–814
91. Gregoriadis G (1993) Liposome technology. CRC Press, Boca Raton, FL
92. Storm G, Crommelin DJA (1998) Liposomes: quo vadis? Pharm Sci Technol To 1:19–31
93. Da Costa G, Mouret L, Chevance S, Le Rumeur E, Bondon A (2007) NMR of molecules interacting with lipids in small unilamellar vesicles. Eur Biophys J Biophy 36:933–942
94. Leland DS (1996) Clinical virology. W.B. Saunders, Philadelphia
95. Tremouilhac P, Strandberg E, Wadhwani P, Ulrich AS (2006) Conditions affecting the re-alignment of the antimicrobial peptide PGLa in membranes as monitored by solid state H-2-NMR. BBA-Biomembranes 1758:1330–1342
96. Afonin S, Durr UHN, Wadhwani P, Salgado J, Ulrich AS (2008) Solid state NMR structure analysis of the antimicrobial peptide gramicidin S in lipid membranes: concentration-dependent re-alignment and self-assembly as a beta-barrel. Top Curr Chem 273:139–154
97. Grage SL, Afonin S, Ulrich AS (2010) Dynamic transitions of membrane-active peptides. Methods Mol Biol 618:183–207
98. Afonin S, Grage SL, Ieronimo M, Wadhwani P, Ulrich AS (2008) Temperature-dependent transmembrane insertion of the amphiphilic peptide PGLa in lipid bilayers; observed by solid state F-19 NMR spectroscopy. J Am Chem Soc 130:16512–16514
99. Strandberg E, Tremouilhac P, Wadhwani P, Ulrich AS (2009) Synergistic transmembrane insertion of the heterodimeric PGLa/magainin 2 complex studied by solid-state NMR. BBA-Biomembranes 1788:1667–1679
100. Arora A, Tamm LK (2001) Biophysical approaches to membrane protein structure determination. Curr Opin Struct Biol 11:540–547
101. Kosol S, Zangger K (2010) Dynamics and orientation of a cationic antimicrobial peptide in two membrane-mimetic systems. J Struct Biol 170:172–179
102. Yeaman MR, Yount NY (2003) Mechanisms of antimicrobial peptide action and resistance. Pharmacol Rev 55:27–55
103. Graham JM, Higgins JA (1998) Molekularbiologische Membrananalyse. Spektrum Akademischer Verlag GmbH, Heidelberg
104. Hanke W, Hanke R (1997) Methoden der Membranphysiologie. Spektrum Akademischer, Heidelberg
105. Shevchenko A, Simons K (2010) Lipidomics: coming to grips with lipid diversity. Nat Rev Mol Cell Bio 11:593–598
106. Stewart JC (1980) Colorimetric determination of phospholipids with ammonium ferrothiocyanate. Anal Biochem 104:10–14
107. Madigan MT, Martinko JM, Parker J (2000) Brock biology of microorganisms. Prentice Hall, Upper Saddle River, NJ
108. Voet DJ, Voet JG, Pratt CW (2010) Lehrbuch der Biochemie. Wiley-VCH, Weinheim
109. Neuhaus FC, Baddiley J (2003) A continuum of anionic charge: structures and functions of D-alanyl-teichoic acids in Gram-positive bacteria. Microbiol Mol Biol R 67:686–723
110. Sutcliffe IC, Shaw N (1991) Atypical lipoteichoic acids of Gram-positive bacteria. J Bacteriol 173:7065–7069
111. Kennedy LD (1974) Teichoic-acid synthesis in Bacillus-stearothermophilus. Biochem J 138:525–535
112. Owen P, Salton MRJ (1975) Succinylated mannan in membrane system of Micrococcus-lysodeikticus. Biochem Biophys Res Commun 63:875–880
113. Powell DA, Duckworth M, Baddiley J (1975) Membrane-associated lipomannan in micrococci. Biochem J 151:387–397
114. Schlegel HG (1992) Allgemeine Mikrobiologie. Georg Thieme Verlag, Stuttgart

115. Papo N, Shai Y (2003) Can we predict biological activity of antimicrobial peptides from their interactions with model phospholipid membranes? Peptides 24:1693–1703
116. Kondejewski LH, Farmer SW, Wishart DS, Kay CM, Hancock REW, Hodges RS (1996) Modulation of structure and antibacterial and hemolytic activity by ring size in cyclic gramicidin S analogs. J Biol Chem 271:25261–25268
117. Ruden S, Hilpert K, Berditsch M, Wadhwani P, Ulrich AS (2009) Synergistic interaction between silver nanoparticles and membrane-permeabilizing antimicrobial peptides. Antimicrob Agents Chemother 53:3538–3540
118. Evans WH, Graham JM (1991) Struktur und Funktion biologischer Membranen. Georg Thieme Verlag, Stuttgart
119. Begemann H, Rastatter J (1993) Klinische Hämatologie. Georg Thieme Verlag, Stuttgart
120. Baake M, Gilles A (1994) Hämatologie. Theorie und Praxis für medizinische Assistenzberufe. GIT Verlag GmbH, Darmstadt
121. Schwoch G, Passow H (1973) Preparation and properties of human erythrocyte-ghosts. Mol Cell Biochem 2:197–218
122. Hanahan DJ, Ekholm JE (1974) The preparation of red cell ghosts (membranes). Methods Enzymol 31:168–172
123. Dodge JT, Mitchell C, Hanahan DJ (1963) The preparation and chemical characteristics of hemoglobin-free ghosts of human erythrocytes. Arch Biochem Biophys 100: 119–130
124. Ieronimo M, Afonin S, Koch K, Berditsch M, Wadhwani P, Ulrich AS (2010) 19F NMR analysis of the antimicrobial peptide PGLa bound to native cell membranes from bacterial protoplasts and human erythrocytes. J Am Chem Soc 132:8822–8824
125. Steck TL (1974) The organization of proteins in the human red blood cell membrane. A review J Cell Biol 62:1–19
126. McLaughlin AC, Cullis PR, Hemminga MA, Hoult DI, Radda GK, Ritchie GA, Seeley PJ, Richards RE (1975) Application of 31P NMR to model and biological membrane systems. FEBS Lett 57:213–218
127. Yeagle PL (1982) 31P nuclear magnetic resonance studies of the phospholipid-protein interface in cell membranes. Biophys J 37:227–239
128. Grobner G, Taylor A, Williamson PT, Choi G, Glaubitz C, Watts JA, de Grip WJ, Watts A (1997) Macroscopic orientation of natural and model membranes for structural studies. Anal Biochem 254:132–138
129. Rockland LB (1960) Saturated salt solutions for static control of relative humidity between 5-degrees-C and 40-degrees-C. Anal Chem 32:1375–1376
130. Afonin S (2004) Structural studies on membrane-active peptides in lipid bilayers by solid state 19F-NMR. PhD thesis, University of Jena
131. Martin HH (1963) Bacterial protoplasts – a review. J Theor Biol 5:1–34
132. Pless DD, Schmit AS, Lennarz WJ (1975) The characterization of mannan of Micrococcus lysodeikticus as an acidic lipopolysaccharide. J Biol Chem 250:1319–1327
133. de Bony J, Lopez A, Gilleron M, Welby M, Laneelle G, Rousseau B, Beaucourt JP, Tocanne JF (1989) Transverse and lateral distribution of phospholipids and glycolipids in the membrane of the bacterium *Micrococcus luteus.* Biochemistry-Us 28:3728–3737
134. Hurley JH, Boura E, Carlson LA, Rozycki B (2010) Membrane budding. Cell 143:875–887
135. Mause SF, Weber C (2010) Microparticles: protagonists of a novel communication network for intercellular information exchange. Circ Res 107:1047–1057
136. Simons M, Raposo G (2009) Exosomes–vesicular carriers for intercellular communication. Curr Opin Cell Biol 21:575–581
137. Beveridge TJ (1999) Structures of Gram-negative cell walls and their derived membrane vesicles. J Bacteriol 181:4725–4733
138. Mashburn-Warren L, Mclean RJC, Whiteley M (2008) Gram-negative outer membrane vesicles: beyond the cell surface. Geobiology 6:214–219

139. Schooling SR, Beveridge TJ (2006) Membrane vesicles: an overlooked component of the matrices of biofilms. J Bacteriol 188:5945–5957
140. Renelli M, Matias V, Lo RY, Beveridge TJ (2004) DNA-containing membrane vesicles of *Pseudomonas aeruginosa* PAO1 and their genetic transformation potential. Microbiol-Sgm 150:2161–2169
141. Kadurugamuwa JL, Beveridge TJ (1995) Virulence factors are released from Pseudomonas-aeruginosa in association with membrane-vesicles during normal growth and exposure to gentamicin – a novel mechanism of enzyme-secretion. J Bacteriol 177:3998–4008
142. Mangoni ML, Rinaldi AC, Di Giulio A, Mignogna G, Bozzi A, Barra D, Simmaco M (2000) Structure-function relationships of temporins, small antimicrobial peptides from amphibian skin. Eur J Biochem 267:1447–1454
143. Matsuzaki K, Murase O, Fujii N, Miyajima K (1996) An antimicrobial peptide, magainin 2, induced rapid flip-flop of phospholipids coupled with pore formation and peptide translocation. Biochemistry-Us 35:11361–11368
144. Blazyk J, Wiegand R, Klein J, Hammer J, Epand RM, Epand RF, Maloy WL, Kari UP (2001) A novel linear amphipathic beta-sheet cationic antimicrobial peptide with enhanced selectivity for bacterial lipids. J Biol Chem 276:27899–27906
145. Steiner V, Schar M, Bornsen KO, Mutter M (1991) Retention behaviour of a template-assembled synthetic protein and its amphiphilic building blocks on reversed-phase columns. J Chromatogr 586:43–50
146. Ferre R, Badosa E, Feliu L, Planas M, Montesinos E, Bardaji E (2006) Inhibition of plant-pathogenic bacteria by short synthetic cecropin A-melittin hybrid peptides. Appl Environ Microbiol 72:3302–3308